

# Methamphetamine Removal from Aquatic Environments by Magnetic Microrobots with Cyclodextrin Chiral Recognition Elements

Paula Mayorga–Burrezo, Carmen C. Mayorga–Martinez, Martin Kuchař, and Martin Pumera\*

The growing consumption of drugs of abuse together with the inefficiency of the current wastewater treatment plants toward their presence has resulted in an emergent class of pollutants. Thus, the development of alternative approaches to remediate this environmental threat is urgently needed. Microrobots, combining autonomous motion with great tunability for the development of specific tasks, have turned into promising candidates to take on the challenge. Here, hybrid urchin-like hematite ( $\alpha$ -Fe<sub>2</sub>O<sub>3</sub>) microparticles carrying magnetite (Fe<sub>3</sub>O<sub>4</sub>) nanoparticles and surface functionalization with organic  $\beta$ -cyclodextrin (CD) molecules are prepared with the aim of on-the-fly encapsulation of illicit drugs into the linked CD cavities of moving microrobots. The resulting mag-CD microrobots are tested against methamphetamine (MA), proving their ability for the removal of this psychoactive substance. A dramatically enhanced capture of MA from water with active magnetically powered microrobots when compared with static passive CD-modified particles is demonstrated. This work shows the advantages of enhanced mass transfer provided by the externally controlled magnetic navigation in microrobots that together with the versatility of their design is an efficient strategy to clean polluted waters.

## 1. Introduction

The 2023 European Drug Report<sup>[1]</sup> issued an alert about the great diversity, availability, and use of drugs of abuse including illicit drugs and misused prescription medicines. Unfortunately, when considering the impact that these psychoactive substances are generating, not only health risks but also an environmental threat must be discussed. They easily penetrate the hydrological cycle as unaltered forms or metabolites excreted after human consumption or as residues from production/distribution activities from the drug market. Hence, drugs of abuse have become an emergent class of pollutants that endangers freshwaters and marine habitats.<sup>[2]</sup> Among them, special attention must be devoted to methamphetamine (MA). The growing consumption of this highly addictive element, as well as its use as a medical treatment for some mental health diseases,<sup>[3]</sup>

P. Mayorga–Burrezo, M. Pumera  
Future Energy and Innovation Laboratory  
Central European Institute of Technology  
Brno University of Technology  
Purkyňova 656/123, Brno CZ-616 00, Czech Republic  
E-mail: [martin.pumera@ceitec.vutbr.cz](mailto:martin.pumera@ceitec.vutbr.cz)

C. C. Mayorga–Martinez  
Center for Advanced Functional Nanorobots  
University of Chemistry and Technology Prague  
Technická 5, Prague 6 166 28, Czech Republic

M. Kuchař  
Forensic Laboratory of Biologically Active Substances  
Department of Chemistry of Natural Compounds  
University of Chemistry and Technology Prague  
Technická 5, Prague 6 166 28, Czech Republic

M. Kuchař  
Department of Experimental Neurobiology  
National Institute of Mental Health  
Topolová 748, Klecany 250 67, Czech Republic

M. Pumera  
Department of Medical Research  
China Medical University Hospital  
China Medical University  
No. 91 Hsueh-Shih Road, Taichung 40402, Taiwan

M. Pumera  
Department of Paediatrics and Inherited Metabolic Disorders  
First Faculty of Medicine  
Charles University Prague  
Ke Karlovu 2, Prague 128 08, Czech Republic

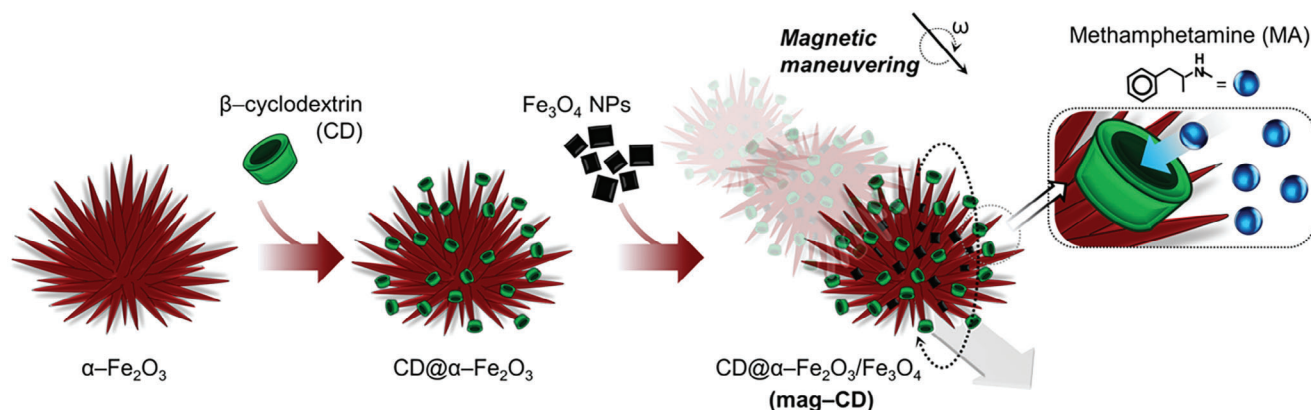
M. Pumera  
Advanced Nanorobots & Multiscale Robotics Lab  
Faculty of Electrical Engineering and Computer Science  
VSB – Technical University of Ostrava  
17 listopadu 2172/15, Ostrava 70800, Czech Republic

M. Pumera  
Department of Chemical and Biomolecular Engineering  
Yonsei University  
50 Yonsei-ro, Seodaemun-gu, Seoul 03722, South Korea

 The ORCID identification number(s) for the author(s) of this article can be found under <https://doi.org/10.1002/smll.202306943>

© 2024 The Authors. Small published by Wiley-VCH GmbH. This is an open access article under the terms of the [Creative Commons Attribution License](https://creativecommons.org/licenses/by/4.0/), which permits use, distribution and reproduction in any medium, provided the original work is properly cited.

DOI: 10.1002/smll.202306943



**Scheme 1.** Magnetic microrobots remove drugs of abuse. Schematic representation of the preparation of  $\beta$ -cyclodextrin (CD)-modified hybrid hematite/magnetite (i.e., mag-CD) microrobots. MA removal is facilitated due to the synergistic combination of magnetic maneuvering and the hydrophobic cavities provided by  $\beta$ -CD functionalization.

has led to the appearance of an increasing number of clandestine manufacturers as well. Despite official guidelines on MA decontamination,<sup>[4,5]</sup> the inefficiency of current remediation methods<sup>[6,7]</sup> has caused the detection of increasing MA concentrations in wastewater analyses in up to 40 European cities in the 2021–2022 period.<sup>[1]</sup> Besides, a harmful effect on aquatic ecosystems has been proved by the behavior alteration of fish.<sup>[8]</sup> In addition, MA residues have been detected in tap water in several European countries,<sup>[6]</sup> turning MA pollution into an additional public health issue. Consequently, it is necessary to test alternative cleaning methods to remediate this situation.

Microrobots enable enhanced mass transfer due to their autonomous motion, great tunability of their surfaces for the development of specific tasks,<sup>[9–14]</sup> and their swarming/collective behavior. Consequently, they are rapidly evolving in their applications for environmental remediation.<sup>[15]</sup> In fact, their action against different residues, from organic dyes<sup>[16,17]</sup> to microplastics,<sup>[18–21]</sup> heavy metals,<sup>[22–24]</sup> hormones,<sup>[25]</sup> or antibiotics<sup>[26,27]</sup> among others, have been discussed. However, the utilization of microrobots for the removal of drugs of abuse remains largely unexplored.<sup>[28]</sup>

Here, we utilize magnetically powered microrobots modified with chiral cyclodextrin (CD) molecules.<sup>[29,30]</sup> CDs are organic supramolecular structures with hydrophobic cavities that provide an optimal environment to form host–guest complexes based on non-covalent interactions. CDs are often used for drug delivery and encapsulation and have also been extensively used for the removal of different water pollutants<sup>[31–33]</sup> including MA.<sup>[34]</sup> In fact, the host–guest complex between CDs and MA has been widely reported in the literature, particularly in analytical chemistry, where CD-based stationary phases of chromatographic techniques are used for the MA separation and subsequent detection.<sup>[35–39]</sup> However, they are scarcely employed in the field of microrobots, being limited to a few proof-of-concept studies performed on enantioselectivity<sup>[40]</sup> and drug delivery.<sup>[41,42]</sup>

This work puts together promising microrobot technology and CD chemistry to deal with the environmental and health threats caused by MA pollution. To this end, hybrid urchin-like hematite ( $\alpha$ - $\text{Fe}_2\text{O}_3$ ) microparticles carrying magnetite ( $\text{Fe}_3\text{O}_4$ ) nanoparticles are combined with CD surface functionalization for MA re-

moval. The iron oxide-based microrobots provide magnetic maneuvering that benefits enhanced mass transfer while CD hydrophobic cavities promote MA capture (Scheme 1).

## 2. Results and Discussion

Hematite microparticles, the most stable iron oxide derivative, were used as backbone material for mag-CD microrobots. To date, hematite-based microrobots showing spheres,<sup>[43]</sup> cubes,<sup>[44]</sup> dendrites,<sup>[45]</sup> or peanut-like<sup>[46]</sup> morphologies have already been explored. The hydrothermal method selected in this work provided original urchin-like shapes with an approximate diameter of  $3.6 \pm 0.9 \mu\text{m}$  (Figure 1A) and a homogeneous distribution of iron and oxygen, their constituent elements (Figure 1B). As depicted in Figure 1C (top), the XRD analysis confirmed a perfect indexation to the  $\alpha$ - $\text{Fe}_2\text{O}_3$  rhombohedral crystal system (100%, ICDD: 01-076-4579), where all peaks were easily identified. The Brunauer–Emmett–Teller (BET) method was used to measure a specific surface area of  $19.3 \text{ m}^2 \text{ g}^{-1}$  (Figure S1, Supporting Information). This value is slightly higher than the one reported for hollow urchin-like hematite particles ( $18.8 \text{ m}^2 \text{ g}^{-1}$ ),<sup>[47]</sup> which is beneficial for their further surface functionalization.

$\beta$ -CD molecules (Figure 1C (central)) were anchored to pristine hematite urchins through an amine modification in line with previous literature<sup>[48]</sup> (Figure S2, Supporting Information, see Experimental Section for further details). FTIR spectra were recorded to gain more insights into the presence of these organic cavities (Figure 1D). In addition to the Fe–O stretching modes detected below  $550 \text{ cm}^{-1}$ ,<sup>[49,50]</sup> new features were observed in the case of the modified urchins and associated with  $\beta$ -CDs: O–H stretching, and C–H asymmetric/symmetric stretching modes were identified at  $3300$  and  $2921 \text{ cm}^{-1}$ , respectively, while the H–O–H bending was found at  $1643 \text{ cm}^{-1}$ . On the other hand, C–O–C asymmetric and symmetric stretching vibrations were associated with the bands at  $1151$  and  $1022 \text{ cm}^{-1}$ , respectively.<sup>[51–53]</sup>

It is known that  $\alpha$ - $\text{Fe}_2\text{O}_3$  hematite-based microrobots respond to relatively weak magnetic fields.<sup>[45,54]</sup> Nonetheless, different chemical/physical factors, such as size, morphology, and vacancies, can alter the magnetic coercivity in  $\alpha$ - $\text{Fe}_2\text{O}_3$  microparticles.<sup>[55–57]</sup> The magnetic properties of the urchin-like

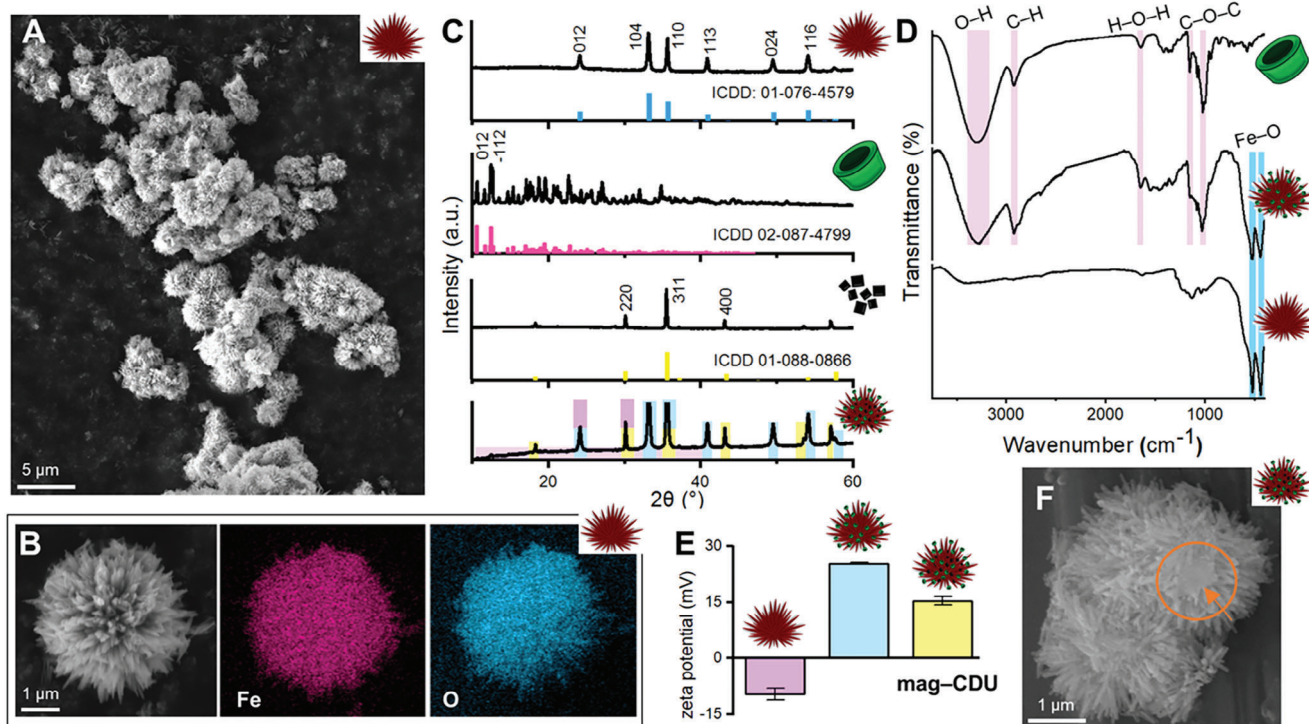


**Figure 1.** Material characterization. A) SEM image of as-prepared -Fe<sub>2</sub>O<sub>3</sub> microrochins, the backbone material for mag-CD microrobots. B) EDS elementary mapping of a single microrochin. C) XRD pattern of mag-CD microrobots (bottom) together with their individual components: -Fe<sub>2</sub>O<sub>3</sub> microrochins (top), CD, and Fe<sub>3</sub>O<sub>4</sub> NPs (central). Additionally, ICDD files are shown. Note a dual color pattern in several peaks in the case of mag-CD microrobots, in line with the different contributions detected (see Figure S1, Supporting Information, for further details). D) FTIR spectra of CD (top), mag-CD microrobots (central), and Fe<sub>2</sub>O<sub>3</sub> microrochins (bottom). E) Zeta potential values recorded through the synthetic process, from the as-prepared -Fe<sub>2</sub>O<sub>3</sub> microrochins to -CD-functionalized intermediates and mag-CD microrobots. F) SEM image of a single mag-CD microrobot highlighting the presence of Fe<sub>3</sub>O<sub>4</sub> NPs.

hematite microparticles ( $\alpha$ -Fe<sub>2</sub>O<sub>3</sub>) and  $\alpha$ -Fe<sub>2</sub>O<sub>3</sub>@CD were analyzed by means of a vibrating sample magnetometer (VSM); however, only insignificant magnetic hysteresis was observed, indicating their low ability to be magnetized (Figure S4, Supporting Information). The surface of the microrochins was modified with commercially available Fe<sub>3</sub>O<sub>4</sub> NPs<sup>21</sup> (Figure S3, Supporting Information) to obtain mag-CD microrobots ( $\alpha$ -Fe<sub>2</sub>O<sub>3</sub>@CD/Fe<sub>3</sub>O<sub>4</sub>). Ferromagnetic behavior was demonstrated by the resulting magnetic hysteresis loop as measured by VSM due to the presence of the Fe<sub>3</sub>O<sub>4</sub> NPs (Figure S4, Supporting Information). Moreover, a positive response was observed when exposed to a permanent magnet (Figure S5, Supporting Information), corroborating once more the magnetic character of mag-CD microrobots. The whole preparation method was monitored by zeta potential measurements (Figure 1E), showing a clear evolution from the pristine urchins to final mag-CD microrobots as follows:  $-10 \pm 2$  mV (Fe<sub>2</sub>O<sub>3</sub>);  $25.4 \pm 0.3$  mV (Fe<sub>2</sub>O<sub>3</sub>@CD);  $15 \pm 1$  mV (Fe<sub>2</sub>O<sub>3</sub>@CD/Fe<sub>3</sub>O<sub>4</sub>). Additionally, Figure 1C (bottom) includes XRD data for mag-CD microrobots, showing all main contributions from Fe<sub>3</sub>O<sub>4</sub> NPs (ICDD: 01-088-0866), as well as the features at  $2\theta < 20^\circ$  that could be associated with  $\beta$ -CDs<sup>[51]</sup> (see Figure S6, Supporting Information for further details). It is also worth mentioning that the original urchin-like morphology was preserved after the functionalization process as demonstrated by the scanning

electron microscope (SEM) images of a mag-CD microrobot in Figure 1F.

The magnetic maneuvering of hybrid mag-CD microrobots under a transversal rotating magnetic field was faced after concluding an exhaustive material characterization. Figures 2 and S7, Supporting Information, and Movies S1–S3, Supporting Information, summarize the most relevant findings on this matter. First, the navigation of a single microrobot under a predefined linear mode was checked using a fixed field intensity of 5 mT and several frequencies (1–5 Hz). Figure 2A (Movie S1, Supporting Information) depicts the clear net displacements recorded in all cases, showing how microrobots covered greater distances with increasing frequency.

Alternative predefined modes, such as perpendicular (Figure 2B and Movie S2 (left), Supporting Information) or random (Figure 2C and Movie S2 (right), Supporting Information), were also explored, proving total spatial control over their navigation. Importantly, different-sized microrobots were observed during the analysis of the different trajectories. The smallest entities were identified as residual Fe<sub>3</sub>O<sub>4</sub> NPs while bigger aggregates of mag-CD microrobots were thought to have been formed due to the electrostatic interactions occurring during their preparation and/or navigation.<sup>[20]</sup> Nonetheless, this size variability did not have any impact on the magnetic maneuvering. On the contrary, harmonized motions following

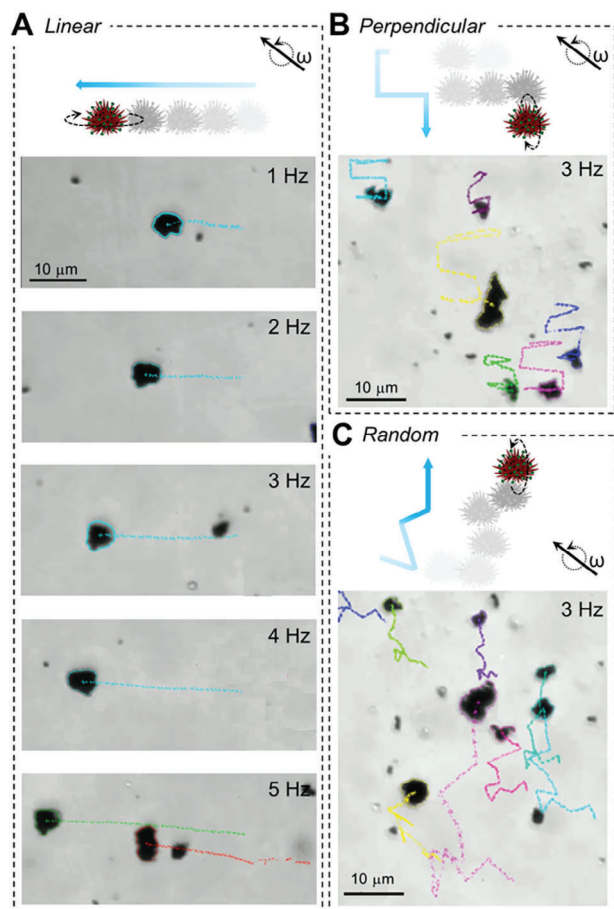


**Figure 2.** Magnetic steering. Schematic representations and time-lapse microscopy images for: A) the predefined linear trajectories of mag-CD microrobots when exposed to a transversal rotatory magnetic field (MF) at an increasing frequency (1–5 Hz,  $t = 5$  s). B) Perpendicular and C) random predefined propulsion modes showing harmonized motions following a swarming effect (3 Hz,  $t = 10$  s). Experimental conditions: solvent =  $\text{H}_2\text{O}$ ; [Tween 20] = 0.1 wt%; MF intensity = 5 mT.

a swarming effect were recorded in all cases. Velocity data were also considered during the motion analysis of mag-CD microrobots and estimated at different frequencies (Movie S3 and Figure S7A, Supporting Information). As expected, higher frequencies resulted in faster navigation, in line with the direct proportionality between both terms up to 6 Hz. Beyond this frequency, the velocity of mag-CD microrobots became unstable and decreased. Therefore, the out-step frequency of the mag-CD microrobots was estimated at 6 Hz. In addition, the performance of the microrobots was evaluated in alternative realistic aqueous media (tap and river water). The microrobots could move freely in both samples (Movie S3, Supporting Information) although some differences in their speed trends were noticed. As depicted in Figure S7B, Supporting Information, faster navigation in tap water was estimated when increasing frequency from 1 to 6 Hz was applied, and similarly in DI water. Nonetheless, a different development was found in river water when no apparent evolution was observed beyond 2 Hz. This finding may be related to the effect that alternative aqueous matrixes and their viscosities

have on the final performance of the microrobots, shifting their out-step frequency.

Finally, the removal of illicit drug residues by mag-CD microrobots was addressed, taking MA as the target pollutant (Figure 3A). A magnetic assay named “dynamic” was carried out with a dispersion of mag-CD microrobots ( $0.8 \text{ mg mL}^{-1}$ ) in a  $200 \text{ ng mL}^{-1}$  MA aqueous solution without further additives. A transversal magnetic rotating field (5 mT, 3 Hz) was applied in this “dynamic assay” for 40 min with a predefined random propulsion mode.<sup>[58]</sup> In addition, high-resolution mass spectroscopy (HRMS) was used to evaluate the fate of MA. Considering a positive atmospheric pressure chemical ionization (APCI) method, the presence of MA was associated with a signal observed at  $m/z = 150.127$  ( $[\text{C}_{10}\text{H}_{15}\text{N}+\text{H}]^+$ ), and the evolution of this feature was related to the action of the microrobots. Interestingly, the

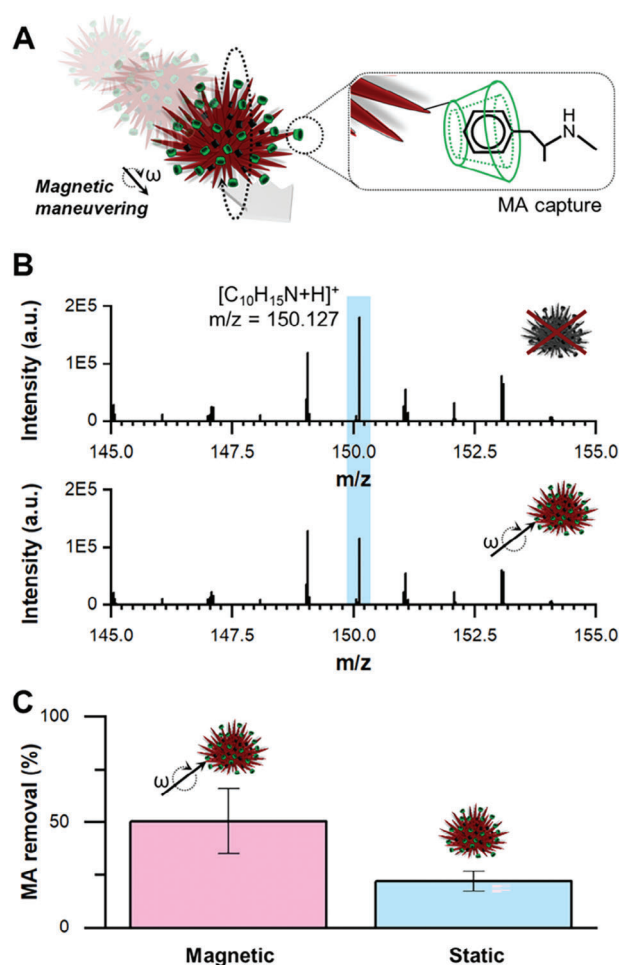


**Figure 3.** Performance of mag-CD microrobots as aquatic cleaners for illicit drug residues. A) Schematic representation of the magnetic navigation of mag-CD microrobots and methamphetamine (MA) capture in the presence of CDs (in green). B) HRMS data detecting the presence of methamphetamine (MA) before (top) and after (bottom) the action of the mag-CD microrobots. C) Comparison between dynamic and static assays. Experimental details: MA signal:  $[\text{C}_{10}\text{H}_{15}\text{N}+\text{H}]^+$ ,  $m/z = 150.127$ ; [MA] =  $200 \text{ ng mL}^{-1}$ ; [mag-CD] =  $0.8 \text{ mg mL}^{-1}$ ; solvent =  $\text{H}_2\text{O}$ ; time = 40 min; MF intensity = 5 mT, frequency = 3 Hz, and a predefined random propulsion mode ( $N = 2$ ).

original MA signal (Figure 3B (top)) was considerably reduced after the performance of mag-CD microrobots (Figure 3B (bottom)), achieving a significant %MA removed:  $50.5 \pm 15.4$ . It is known that basic pH values like 10–11 enhance the kinetics of the CD-MA host-guest complexes.<sup>[34,59]</sup> Nonetheless, the performance of the mag-CD microrobots was analyzed without optimizing this parameter, in line with the actual environments of raw waters where the micromotors would be tested as micro-cleaners. It is worth emphasizing that the presence of MA in surface water, potable water, and wastewater is detected at amounts of several  $\text{ng L}^{-1}$  or less.<sup>[2]</sup> This work demonstrated 50% MA removal by the action of mag-CD microrobots from a  $200 \text{ ng mL}^{-1}$  initial MA solution, which differs by three orders of magnitude from the values previously found. In addition, because only 40 min were needed for this achievement, it is safe to say that these microrobots would guarantee a successful performance in real polluted waters.

A “static assay” was then prepared to assess the impact of the magnetic maneuvering on the %MA removal. Thus, the same experimental conditions were kept but without applying a transversal magnetic rotating field. A comparison between the dynamic and the static assays, depicted in Figure 3C, clearly reveals a superior response of the one involving the magnetic motion, with an estimated increment of 56.24%. In this sense, the mag-CD microrobots would act as externally controlled micromixers able to generate an enhanced mass transfer that promotes the MA removal through the establishment of host-guest supramolecular interactions with CD cavities.

We further investigated the impact of CDs on the performance of mag-CD microrobots for MA removal. A “control-blank” sample of magnetic microurchins without CD functionalization was prepared for the experiment and their activity was compared to that of mag-CD microrobots (Figure S8, Supporting Information). Moreover, instead of a transversal magnetic rotating field, an external mechanical shaker was used to contextualize the magnetic navigation of the microrobots. A negligible performance of the unfunctionalized microparticles was observed after 40 min. Thus, the MA capture was undoubtedly related to the hydrophobic cavities of the CD placed on the surface of mag-CD microrobots (Figure 3A). It is important to mention that the percentage yield of MA removal was  $99.2 \pm 0.1\%$  when mag-CD microrobots were combined with the external shaker. A higher efficiency was estimated in this assay due to the enhanced mass transfer provided by the external shaker. Nonetheless, with real applicability in mind, the intrinsic motion of the mag-CD microrobots can be considered a more interesting approach. As demonstrated in this work, they can produce a mass transfer high enough to decrease MA concentration ( $\text{ng L}^{-1}$ ) from wastewater treatment plants. In addition, lower implementation costs would be needed compared to those associated with the use of external shakers for high volumes of treated water. In terms of the reusability of the mag-CD microrobots, two main factors should be mentioned without considering the stability of the CD-functionalization, which is guaranteed by covalent bonds<sup>[34,48]</sup> (Figure S2, Supporting Information). On the one hand, there are the stability of the host-guest complexes between CDs and MA. In this regard, CDs have been reported as a key component of extraction phases for the determination of MA in biological samples like saliva<sup>[34]</sup> or urine.<sup>[32]</sup> An easy release of the MA from the hydrophobic cavities of CDs has

been described in those cases, being that the MA rapidly eluted to be further analyzed. On the other hand, the magnetic motion must be preserved for the mag-CD microrobots to accomplish their final task. SEM images were obtained after the MA removal to address this point. As depicted in Figure S9, Supporting Information,  $\text{Fe}_3\text{O}_4$  NPs are still observed in the mag-CD microrobots to ensure their magnetic navigation. Consequently, it is clear that the microrobots are reusable.

Finally, the performance of the mag-CD microrobots should be compared with current tertiary or advanced treatments implemented in wastewater treatment plants for MA removal.<sup>[7]</sup> This work demonstrates that the performance of the mag-CD microrobots is not limited by specific working conditions, such as pH, as in the case of Fenton reaction treatments. Unlike ozonation, their activity does not involve a transformation to products of higher toxicity and risk for aquatic life, and it occurs in a fuel-free context. Additionally, the magnetic response in mag-CD microrobots also ensures easy retrieval following the completion of their specific tasks, avoiding the separation and recovery issues associated with photocatalytic degradations based on  $\text{TiO}_2$ . Thus, microrobots provide an eco-friendly approach to MA removal.

### 3. Conclusion

The emergent environmental threat originating from residues from drugs of abuse is discussed in the context of microrobots and their applicability for water remediation. Mag-CD microrobots, made of a hybrid inorganic hematite/magnetite core together with a surface functionalization with CD, have been presented and used for the removal of MA as the target pollutant. From the comparison of the static and dynamic assays, a synergistic combination of the magnetic motion with the hydrophobic cavities from CDs has been proved, with an estimated enhanced performance for MA removal of 56.24%. Moreover, no adsorption capabilities were detected without CD functionalization. This work highlights how the successful performance of microrobots should be equally attributed to i) autonomous navigation, ii) enhanced mass transfer, and iii) an accurate design involving the functionalization of a specific task.

### 4. Experimental Section

**Materials:** Iron(III) chloride hexahydrate ( $\text{FeCl}_3 \cdot 6\text{H}_2\text{O}$ ), iron(II,III) oxide, sodium acetate ( $\text{CH}_3\text{COONa}$ ), (3-aminopropyl) triethoxysilane (APTES), and tetraethyl orthosilicate (TEOS) were purchased from Sigma-Aldrich (Merck, Germany). Sodium sulfate anhydrous ( $\text{Na}_2\text{SO}_4$ ) was procured from Lach-ner, s.r.o. (Czech Republic) and beta-Cyclodextrin hydrate (b-CD, 95%) from abcr GmbH (Germany). All the reactants were used as provided.

**Synthesis of mag-CD Microrobots—Microurchins:** A solvothermal method was followed for the preparation of  $\alpha\text{-Fe}_2\text{O}_3$  urchin-like microparticles.<sup>[47]</sup> Briefly, an aqueous solution of  $\text{Na}_2\text{SO}_4$  (0.1 M, 10 mL) was added dropwise to an aqueous  $\text{FeCl}_3$  solution (0.5 M, 2 mL) under vigorous stirring. After 10 min, a dropwise addition of 8 mL of Milli-Q  $\text{H}_2\text{O}$  to the mixture was carried out keeping the stirring conditions. The mixture was transferred to a Teflon-lined autoclave to perform a hydrothermal reaction for 12 h at  $140^\circ\text{C}$ . The resulting material was washed with Milli-Q  $\text{H}_2\text{O}$  and centrifuged (10 min,  $\times 5$ ), and then dried

overnight (85 °C). A tubular furnace was used for the annealing of the samples at 600 °C for 120 min (1 °C min<sup>-1</sup>).

**Synthesis of mag-CD Microrobots—CD-Functionalized Microrouchins:** An amine-functionalization with APTES was considered as a first step to achieve a surface modification with CD<sup>[48]</sup> (Figure S2, Supporting Information). A 1 mg mL<sup>-1</sup> dispersion of  $\alpha$ -Fe<sub>2</sub>O<sub>3</sub> microparticles in Milli-Q H<sub>2</sub>O (pH 4, sodium acetate buffer) was prepared and stirred at 60 °C. After 60 min, EtOH and APTES were added to the dispersion, keeping a 1:1 (EtOH):0.7 (APTES) ratio, and mechanically shaken overnight at room temperature. NH<sub>2</sub>-U microparticles were washed with EtOH and centrifuged (10 min,  $\times$ 5), and then dried overnight in an oven at 60 °C. Afterward, NH<sub>2</sub>-U microparticles were dispersed in a 1:2.75 DMF:THF solution where b-CDs were then added in a 1:2 NH<sub>2</sub>-U:CD ratio. The dispersion was mechanically shaken overnight at room temperature to promote interaction between the hydroxyl and amine groups from b-CDs and NH<sub>2</sub>-U. The resulting microparticles were washed with THF and centrifuged (10 min,  $\times$ 5), and then dried in an oven at 70 °C.

**Mag-CD Microrobots:** A 1 mg mL<sup>-1</sup> dispersion of commercially available Fe<sub>3</sub>O<sub>4</sub> nanoparticles was prepared in pH 4, sodium acetate buffer. In addition, a 3 mg mL<sup>-1</sup> dispersion of CD-functionalized microrouchins was prepared in pH 4, sodium acetate buffer, and mixed with 0.35 mL from the Fe<sub>3</sub>O<sub>4</sub> NPs dispersion. The mixture was mechanically shaken for 30 min to promote the electrostatic interactions between both components.<sup>[20]</sup> Final mag-CD microrobots were washed with Milli-Q H<sub>2</sub>O ( $\times$ 3) and collected with the help of a permanent magnet.

**Morphological and Structural Characterization for mag-CD Microrobots:** A field-emission SEM was used to obtain SEM images and a coupled energy-dispersive X-ray spectrometer for EDX elementary mappings. XRD measurements were run in an X-ray diffractometer (Bruker, Germany). In the case of zeta potential, a ZETASIZER PRO (Malvern) with a folded Capillary Zeta Cell was used for the three replicas. Samples for FTIR were in the spectral range 4000–400 cm<sup>-1</sup>, resolution 4 cm<sup>-1</sup>, number of spectra accumulations = 64, Happ–Genzel apodization. ATR correction was performed. The spectra were corrected for carbon dioxide and humidity in the optical path. The region of the spectra from 2400 to 1900 cm<sup>-1</sup> was cut out due to the diamond crystal artifact.

**Motion of Microrobots:** A transversal rotating magnetic field was used that comprised a homemade 3D-printed six-coil system attached to the microscope table and a homemade magnetic field controller. The magnetic intensity used in all the experiments was 5 mT and frequencies between 0 and 6 Hz were screened.

**MA Detection:** Mag-CD microrobots (0.8 g mL<sup>-1</sup>) were dispersed in aqueous MA solutions (200 ng mL<sup>-1</sup>). The concentration of the microrobots was selected as a result of an optimization process while that for MA was chosen in line with previous literature.<sup>[28]</sup> At least two replicas of all the assays were done using VWR Tissue Culture plates (24 wells, sterile). The transversal rotating magnetic field (5 mT) was provided by a homemade 3D-printed six-coil system tuned with a homemade controller. As mentioned in Figure S7B, Supporting Information, the out-step frequency of mag-CD microrobots could be shifted depending on the viscosity of the selected aqueous media, being 6 Hz for DI and tap water, and  $\approx$ 2 Hz for river water. As a result, an intermedial frequency (3 Hz) was set in order to i) maximize the mass transfer promoted by the magnetic navigation of the microcleaners and ii) favor the capture of MA molecules inside the hydrophobic cavities of the CDs in the mag-CD microrobots.<sup>[58]</sup> A predefined random propulsion mode was used. Consequently, the possible accumulation of microrobots associated with unidirectional modes was prevented.<sup>[58,60]</sup> Alternatively, a Vortex mixer was used in the case of external stirring. An optimized duration of 40 min was used for all assays. HRMS data were acquired before and after the assays to check the evolution of the MA signal. An LTQ Orbitrap Velos-hybrid ion-trap-orbitrap MS spectrometer was selected to this end, considering an ion-max as an ion source and APCI positive for ionization. Spray current 4  $\mu$ A; source temperature 350 °C; capillary temperature 300 °C; sheath gas (flow units): 40; aux gas (flow units): 10; sweep gas (flow units): 0; mode: FTMS resolution (FWHM): 30 000; lock mass 391.2842 Da (diisooctyl phthalate); and scan: 50–500 Da.

## Supporting Information

Supporting Information is available from the Wiley Online Library or from the author.

## Acknowledgements

The work was supported by the ERDF/ESF project TECHSCALE (No. CZ.02.01.01/00/22\_008/0004587). This research was co-funded by the European Union under the REFRESH – Research Excellence For REgion Sustainability and High-tech Industries project number CZ.10.03.01/00/22\_003/0000048 via the Operational Programme Just Transition. This work was supported by the Ministry of Education, Youth and Sports (Czech Republic) grant LL2002 under the ERC CZ program. This work was supported by funds from the Ministry of Health of the Czech Republic (NU21-08-00407). The authors thank O. Zivotsky for magnetic properties measurements.

Open access publishing facilitated by Vysoke uceni technicke v Brne, as part of the Wiley - CzechELib agreement.

## Conflict of Interest

The authors declare no conflict of interest.

## Data Availability Statement

The data that support the findings of this study are available from the corresponding author upon reasonable request.

## Keywords

illicit drugs, iron oxides, magnetic actuation, water remediation

Received: August 13, 2023

Revised: January 7, 2024

Published online: January 18, 2024

- [1] European Monitoring Centre for Drugs and Drug Addiction, European Drug Report 2023: Trends and Developments, <https://www.emcdda.europa.eu/publications/european-drug-report/2023-en> (accessed: May 2023).
- [2] R. Y. Krishnan, S. Manikandan, R. Subbaiya, M. Biruntha, R. Balachandar, N. O. Karmegam, *Chemosphere* **2023**, *311*, 137091.
- [3] G. Perugi, G. Vannucchi, F. Bedani, E. Favaretto, *Curr. Psychiatry Rep.* **2017**, *19*, 7.
- [4] Utah Department of Health, UDH, Development of Utah's methamphetamine decontamination standard, Salt Lake City, Utah, **2015**.
- [5] Ministry of Business, Innovation and Employment, New Zealand Government, Wellington, **2017**.
- [6] L. Muñiz-Bustamante, N. Caballero-Casero, S. Rubio, *Environ. Int.* **2022**, *164*, 107281.
- [7] M. Ponce-Arguello, V. Abad-Sarango, T. Crisanto-Perrazo, T. Toulkeridis, *Water* **2022**, *14*, 1807.
- [8] P. Horký, R. Grabic, K. Grabicová, B. W. Brooks, K. Douda, O. Slavik, P. Hubená, E. M. S. Santos, T. Randák, *J. Exp. Biol.* **2021**, *224*, jeb242145.
- [9] M. Ussia, M. Pumera, *Chem. Soc. Rev.* **2022**, *51*, 1558.
- [10] F. Ji, Y. Wu, M. Pumera, L. Zhang, *Adv. Mater.* **2023**, *35*, 2203959.
- [11] B. Wang, S. Handschuh-Wang, J. Shen, X. Zhou, Z. Guo, W. Liu, M. Pumera, L. Zhang, *Adv. Mater.* **2023**, *35*, 2205732.

- [12] J. Yong, A. S. Mellick, J. Whitelock, J. Wang, K. Liang, *Adv. Mater.* **2023**, 35, 2205746.
- [13] F. Zhang, J. Zhuang, Z. Li, H. Gong, B. E.-F. de Ávila, Y. Duan, Q. Zhang, J. Zhou, L. Yin, E. Karshalev, W. Gao, V. Nizet, R. H. Fang, L. Zhang, J. Wang, *Nat. Mater.* **2022**, 21, 1324.
- [14] J. Llacer-Wintle, A. Rivas-Dapena, X. Chen, E. Pellicer, B. J. Nelson, J. Puigmartí-Luis, S. Pané, *Adv. Mater.* **2021**, 33, 2102049.
- [15] M. Urso, M. Ussia, M. Pumera, *Nat. Rev. Bioeng.* **2023**, 1, 236.
- [16] X. Zhang, W. Xie, S. Du, H. Wang, Z. Zhang, *Langmuir* **2022**, 38, 4389.
- [17] L. Xu, D. Gong, N. Celi, J. Xu, D. Zhang, J. Cai, *Appl. Surf. Sci.* **2022**, 579, 152165.
- [18] J. Kim, C. C. Mayorga-Martinez, M. Pumera, *Nat. Commun.* **2023**, 14, 935.
- [19] M. Urso, M. Ussia, F. Novotný, M. Pumera, *Nat. Commun.* **2022**, 13, 3573.
- [20] P. Mayorga-Burrezo, C. C. Mayorga-Martinez, M. Pumera, *J. Colloid Interface Sci.* **2023**, 643, 447.
- [21] M. Urso, M. Pumera, *Adv. Funct. Mater.* **2022**, 32, 2112120.
- [22] J. Yang, Y. Liu, J. Li, M. Zuo, W. Li, N. Xing, C. Wang, T. Li, *Appl. Mater. Today* **2021**, 25, 101190.
- [23] K. Villa, C. L. Manzanares Palenzuela, Z. Sofer, S. Matejková, M. Pumera, *ACS Nano* **2018**, 12, 12482.
- [24] J. V. Vaghasiya, C. C. Mayorga-Martinez, S. Matějková, M. Pumera, *Nat. Commun.* **2022**, 13, 1026.
- [25] L. Dekanovsky, B. Khezri, Z. Rottnerova, F. Novotny, J. Plutnar, M. Pumera, *Nat. Mach. Intell.* **2020**, 2, 711.
- [26] C. M. Oral, M. Ussia, M. Pumera, *Small* **2022**, 18, 2202600.
- [27] E. Ma, K. e Wang, Z. Hu, H. Wang, *J. Colloid Interface Sci.* **2021**, 603, 685.
- [28] Y. S. Kochergin, K. Villa, A. Nemeškalová, M. Kuchař, M. Pumera, *ACS Nano* **2021**, 15, 18458.
- [29] H. Zhou, C. C. Mayorga-Martinez, S. Pané, L. Zhang, M. Pumera, *Chem. Rev.* **2021**, 121, 4999.
- [30] H. Zhou, C. C. Mayorga-Martinez, M. Pumera, *Small Methods* **2021**, 5, 2100230.
- [31] S. E. Z. Syeda, D. Nowacka, M. S. Khan, A. M. Skwierawska, *Polymers* **2022**, 14, 2341.
- [32] B. Tian, S. Hua, Y. Tian, J. Liu, *Environ. Sci. Pollut. Res.* **2021**, 28, 1317.
- [33] K. Uekama, F. Hirayama, T. Irie, *Chem. Rev.* **1998**, 98, 2045.
- [34] M. T. García-Valverde, M. L. Soriano, R. Lucena, S. Cárdenas, *Anal. Chim. Acta* **2020**, 1126, 133.
- [35] Y. Makino, A. Suzuki, T. Ogawa, O. Shiota, *J. Chromatogr. B* **1999**, 729, 97.
- [36] K. Lemr, D. Jirovský, J. Ševčík, *J. Liq. Chromatogr. Relat. Technol.* **1996**, 19, 3173.
- [37] Y. J. Heo, Y. S. Whang, M. K. In, K.-J. Lee, *J. Chromatogr. B* **2000**, 741, 221.
- [38] R. Iio, S. Chinaka, N. Takayama, K. Hayakawa, *Anal. Sci.* **2005**, 21, 15.
- [39] A. M. Rizzi, R. Hirz, S. Cladrowa-Runge, H. Jonsson, *Chromatographia* **1994**, 39, 131.
- [40] J. Muñoz, M. Urso, M. Pumera, *Angew. Chem., Int. Ed.* **2022**, 61, 202202690.
- [41] M. Ziemyte, A. Escudero, P. Díez, M. D. Ferrer, J. R. Murguía, V. Martí-Centelles, A. Mira, R. Martínez-Mañez, *Chem. Mater.* **2023**, 35, 4412.
- [42] D. Wang, C. Gao, C. Zhou, Z. Lin, Q. He, *Research* **2020**, 2020, 3676954.
- [43] X. Peng, M. Urso, M. Pumera, *Small Methods* **2021**, 5, 2100617.
- [44] X. Peng, M. Urso, M. Ussia, M. Pumera, *ACS Nano* **2022**, 16, 7615.
- [45] X. Peng, M. Urso, J. Balvan, M. Masarik, M. Pumera, *Angew. Chem., Int. Ed.* **2022**, 61, 202213505.
- [46] J. Palacci, S. Sacanna, A. Vatchinsky, P. M. Chaikin, D. J. Pine, *J. Am. Chem. Soc.* **2013**, 135, 15978.
- [47] F. Zhang, H. Yang, X. Xie, L. Li, L. Zhang, J. Yu, H. Zhao, B. Liu, *Sens. Actuators, B* **2009**, 141, 381.
- [48] D. Chen, Y. Shen, S. Wang, X. Chen, X. Cao, Z. Wang, Y. Li, *J. Colloid Interface Sci.* **2021**, 589, 217.
- [49] A. Mirzaei, K. Janghorban, B. Hashemi, S. Hosseini, M. Bonyani, S. Leonardi, A. Bonavita, G. Neri, *Process. Appl. Ceram.* **2016**, 10, 209.
- [50] M. Farahmandjou, F. Soflaee, *Phys. Chem. Res.* **2015**, 3, 191.
- [51] R. L. Abarca, F. J. Rodríguez, A. Guarda, M. J. Galotto, J. E. Bruna, *Food Chem.* **2016**, 196, 968.
- [52] S. Amani, A. Bagheri Garmarudi, N. Rahmani, M. Khanmohammadi, *RSC Adv.* **2019**, 9, 32348.
- [53] H. Rachmawati, C. A. Edityaningrum, R. Mauludin, *AAPS Pharm-SciTech* **2013**, 14, 1303.
- [54] M. Urso, M. Ussia, M. Pumera, *Adv. Funct. Mater.* **2021**, 31, 2101510.
- [55] M. Aslam, M. T. Qamar, A. U. Rehman, M. T. Soomro, S. Ali, I. M. I. Ismail, A. Hameed, *Appl. Surf. Sci.* **2018**, 451, 128.
- [56] L. Cao, Y. Zeng, Z. Ye, Z. Wang, Y. Zhang, L. Zhao, C. Li, C. Zhang, *New J. Chem.* **2017**, 41, 6436.
- [57] Q. Liu, V. Barrón, J. Torrent, H. Qin, Y. Yu, *Phys. Earth Planet. Inter.* **2010**, 183, 387.
- [58] P. Mayorga-Burrezo, C. C. Mayorga-Martinez, J. Kim, M. Pumera, *Chem. Eng. J.* **2022**, 446, 137139.
- [59] J. Zhou, Z. Zeng, *Anal. Chim. Acta* **2006**, 556, 400.
- [60] J. Kim, C. C. Mayorga-Martinez, J. Vyskocil, D. Ruzek, M. Pumera, *Appl. Mater. Today* **2022**, 27, 101402.